

Perinatal or Adult *Nf1* Inactivation Using Tamoxifen-Inducible *PlpCre* Each Cause Neurofibroma Formation

Debra A. Mayes¹, Tilat A. Rizvi¹, Jose A. Cancelas^{1,3}, Nathan T. Kolasinski¹, Georgianne M. Ciraolo², Anat O. Stemmer-Rachamimov⁴, and Nancy Ratner¹

Abstract

Plexiform neurofibromas are peripheral nerve sheath tumors initiated by biallelic mutation of the NF1 tumor suppressor gene in the Schwann cell lineage. To understand whether neurofibroma formation is possible after birth, we induced *Nf1* loss of function with an inducible proteolipid protein Cre allele. Perinatal loss of *Nf1* resulted in the development of small plexiform neurofibromas late in life, whereas loss in adulthood caused large plexiform neurofibromas and morbidity beginning 4 months after onset of *Nf1* loss. A conditional EGFP reporter allele identified cells showing recombination, including peripheral ganglia satellite cells, peripheral nerve S100 β + myelinating Schwann cells, and peripheral nerve p75+ cells. Neurofibromas contained cells with Remak bundle disruption but no recombination within GFAP+ nonmyelinating Schwann cells. Extramedullary lymphohematopoietic expansion was also observed in *PlpCre;Nf1^{fl/fl}* mice. These tumors contained EGFP+/Sca-1+ stromal cells among EGFP-negative lympho-hematopoietic cells indicating a noncell autonomous effect and unveiling a role of *Nf1*-deleted microenvironment on lympho-hematopoietic proliferation *in vivo*. Together these findings define a tumor suppressor role for *Nf1* in the adult and narrow the range of potential neurofibroma-initiating cell populations. *Cancer Res*; 71(13); 4675–85. ©2011 AACR.

Introduction

Neurofibromatosis type 1 (NF1) is an autosomal dominant inherited disease, affecting approximately 1:3000 individuals worldwide (1). Disease manifestations are observed after mutation or loss of *NF1* in diverse cells and tissues. Common findings include learning and memory difficulties, and optic pathway gliomas (2–3). Rarer manifestations include juvenile myelomonocytic leukemia (JMML) (4–6), a myelodysplastic/myeloproliferative neoplasm characterized by monocytosis, lymphadenopathy, and hepatosplenomegaly.

Most NF1 patients (>90%) develop tumors within the peripheral ganglia, peripheral, and/or cranial nerves called neurofibromas, composed of cell types including neuronal axons, fibroblasts, perineurial cells, Schwann cells, and mast cells (7). Homozygous loss of *NF1* is present only within the Schwann cell compartment (8–10) indicating that cells within the Schwann cell lineage are necessary for neurofibroma

formation. In humans, plexiform neurofibromas can be congenital, suggesting a possible role for a developing Schwann cell in neurofibroma formation. However, the cell(s) of origin for neurofibroma formation within the Schwann cell lineage remain unclear.

Neural crest cells develop into Schwann cell precursors between E11 and E13 in mouse sciatic nerve, and Schwann cells by E18 (11–12). Progenitors identified after the establishment of the dorsal root ganglia (DRG) have more limited self-renewal and differentiation potential than neural crest stem cells (13–17). Schwann cells differentiate in close association with the axons of peripheral nerves. Those Schwann cells associated with neuronal cell bodies form satellite cells that express either S100 β or GFAP. Schwann cells ensheathing multiple small axons in peripheral nerves are GFAP+ nonmyelinating Schwann cells, whereas Schwann cells associating with single large axons form myelin and express S100 β and periaxin (18). Neurofibroma initiating cells may be committed glial cells, de-differentiated Schwann cells, and/or post-crest progenitor cells.

Nf1^{-/-} mouse embryos die by E13.5 due to abnormal heart development and *Nf1*^{+/-} mice do not develop neurofibromas (19–20). Loss of *Nf1* in animal models using neural crest drivers *Wnt1-Cre* (E9.5), *Mpz-Cre* (E9.5–10.5), and *Pax3-Cre* (E10.5) did not result in neurofibroma formation (21). These findings suggested that a post-crest target cell(s) drives neurofibroma formation; therefore, several laboratories targeted *Nf1* loss to Schwann cell populations after neural crest migration. In a pioneering study a *Krox20-Cre* driver line, which expresses within boundary cap cells at E10.5 and later in Schwann cells in peripheral nerves, caused genetically

Authors' Affiliations: ¹Experimental Hematology and Cancer Biology, ²Pathology, Cincinnati Children's Hospital Medical Center; ³Hoxworth Blood Center, University of Cincinnati, Cincinnati, Ohio; and ⁴Department of Pathology, Massachusetts General Hospital and Harvard Medical School, Boston, Massachusetts

Note: Supplementary data for this article are available at Cancer Research Online (<http://cancerres.aacrjournals.org/>).

Corresponding Author: Nancy Ratner, Experimental Hematology and Cancer Biology, Cincinnati Children's Hospital Medical Center, Cincinnati, OH. Phone: 513-636-9469; Fax: 513-803-1083; E-mail: nancy.ratner@cchmc.org

doi: 10.1158/0008-5472.CAN-10-4558

©2011 American Association for Cancer Research.

engineered mice (GEM) neurofibroma formation (22). A *PO_A-Cre*+ driver line in which loss of *Nf1* begins in neural crest at E9.5 with robust expression at E12.5 also enabled neurofibroma formation (23). Loss of *Nf1* in embryonic Schwann cells (E12.5) also caused neurofibroma formation (24). Thus cell(s) developing at or after the embryonic Schwann cell stage of development initiate neurofibroma formation.

Peripheral nerve Remak bundles containing small diameter axons ensheathed by a single Schwann cell are disrupted in all neurofibroma models. In contrast, myelinated axons appear relatively spared. This led to the suggestion that nonmyelinating Schwann cell are tumor-initiating cells within neurofibromas (23).

Myelin proteolipid protein (Plp) is a component of the Schwann cell myelin sheath (25). We used a tamoxifen-inducible *PlpCre* driver line [Plp-Cre-ERT (designated *PlpCre* throughout)] to test the potential role of *Nf1* loss within Plp-expressing cells in neurofibroma formation (26), inducing *Nf1* loss after birth or in adult animals. We report that *Nf1* inactivation at either age results in neurofibroma formation. While Remak bundle disruption is shown within the neurofibromas, GFAP+ nonmyelinating Schwann cells do not show *Nf1* inactivation.

Materials and Methods

Mouse husbandry

Cincinnati Children's Hospital Research Foundation animal care and use committee approved all animal use. Mice were housed in a temperature- and humidity-controlled vivarium on a 12-hour light-dark cycle with free access to food and water.

Mouse strains

Nf1^{flox/+} mice on a mixed 129/B1/6 background (22) were mated to female tamoxifen-inducible *PlpCre* C57Bl6 mice (26). *PlpCre;Nf1^{fl/fl}*+ mice were bred to mice containing a CMV- β actin loxP flanked CAT gene upstream of the enhanced green fluorescent protein cassette (27).

Perinatal tamoxifen injections

Tamoxifen (100 mg) was dissolved in 1 ml of ethanol and 9 mls of sunflower seed oil. Intraperitoneal (i.p.) tamoxifen injection (1 mg/100 μ L) was twice a day for 3 consecutive days to lactating mothers, administering tamoxifen to pups through the mother's milk, beginning when pups were 1 day old. Dose-limiting toxicity was pup trembling and occasional mortality, when tamoxifen was provided twice a day for >3 days. Tamoxifen injection once daily for 3 or 5 days to the mother failed to cause peripheral nerve recombination.

Adult tamoxifen injections

One hundred microliters (1 mg/100 μ L) was administered i.p. once-or-twice-a-day for 3 consecutive days. Tamoxifen administration once daily for 3 or 5 consecutive days did not result in significant adult peripheral nerve recombination. We dosed twice a day for 3 consecutive days.

Genotyping and recombination and survival studies

Mice were genotyped by PCR (22, 26, 27). *Nf1* recombination was determined 30 days after tamoxifen injections using PCR (22). *PlpCre;Nf1^{fl/fl}* mice were euthanized when they became paralyzed, failed to groom, had obvious weight loss, or developed tumor masses.

Tissue processing

We administered Brdu i.p. (50 mg/kg body weight) 3 times at 2-hour intervals. Two hours later, we anesthetized mice and perfused with ice cold 4% paraformaldehyde. Tissues were removed and photographed on a Leica MZFL111 microscope, then post-fixed in 4% paraformaldehyde overnight for paraffin sectioning or for an hour with transfer to 20% sucrose for frozen sectioning. For electron microscopy, we perfused mice with 4% paraformaldehyde and 2.5% glutaraldehyde, post-fixed in the same fixative overnight, and then transferred tissues to 0.175 mol/L cacodylate buffer, osmicated, dehydrated, and embedded in Embed 812 (Ladd Research Industries). Ultrathin sections were stained in uranyl acetate and lead citrate and viewed on a Hitachi Model H-7600 microscope.

Histology

Paraffin sections were processed for H&E to examine tissue structure or stained with Toluidine Blue to identify mast cells. An *in vitro* Brdu staining kit monitored proliferation (Invitrogen). Biotinylated secondary antibodies were used at 1:200 (Vector), together with an ABC kit to visualize immunoreactivity (Vector Labs).

Antibodies

Cryostat sections were air dried and processed for immunohistochemistry using markers for EGFP (chicken GFP 1:2000; Millipore), myelinating Schwann cells [rabbit S100 β 1:25,000 for fluorescence and 1:30,000 for 3,3' diaminobenzidine (DAB); DAKO], nonmyelinating Schwann cells (rabbit GFAP 1:500; DAKO), Schwann cells with glutathione synthase (rabbit GS 1:250; Santa Cruz Biotech), mesenchymal cells (Sca-1 1:200; clone D7, BD-Pharmingen). Fluorescent secondary antibodies were used at 1:200 (Jackson Immuno Labs) except for Alexa 594 at 1:800 (rabbit or mouse; Invitrogen). Histomount or Fluoromount G was used to coverslip DAB or fluorescent sections, respectively. Fluorescent images were captured on a Zeiss Axiovert 200 M microscope using a 40 \times Plan-NEO FLUAR objective, Hamamatsu Orca ER camera, and ImageJ software.

Complete blood counts and flow cytometry analysis

Peripheral blood counts were carried out in a Hemavet counter (Drew Scientific). Blood smears were stained with Diff-Quick for manual counts. Flow cytometry analysis used CD45R/B-220 (clone RA3-6B2)-Pacific Blue, CD3e (clone 145-2C11)-PerCP-Cy5.5, Mac-1 (CD11b, clone M1/70)-PE, Gr-1/Ly6C-G (RB6-8C5)-APC-Cy7 and CD117 (ACK45)-APC (Becton Dickinson) and analyzed for coexpression of EGFP on an alive gate selected based on light scatter parameters in a FACS Canto flow cytometer (Becton Dickinson).

Statistical analyses

Kaplan–Meier survival curves were created using GraphPad Prism software and Log-rank Mantel–Cox Tests. Counting of Schwann cells and satellite cells was carried out on at least 150–300 EGFP+ cells per area per animal from 3–5 animals per genotype. Two-way *t*-tests were carried out on complete blood count (CBC) X Blood Smear counts and immunoreactive cell counts with a significance cutoff of $P < 0.05$.

Results

Postnatal (P1–3) loss of *Nf1* in *PlpCre;Nf1fl/fl* mice causes early and later mortality

To test whether loss of *Nf1* within postnatal cells elicits tumors *in vivo*, we chose a tamoxifen-inducible *PlpCre* driver. Survival was monitored after postnatal (1–3) tamoxifen exposure within *PlpCre* mice and showed two phases of mortality (Fig. 1A; $P < 0.0001$). Seven of 36 *PlpCre;Nf1fl/fl* animals died when they were 5–7 months old, displaying hematopoietic lesions characteristic of lymphoma (7/36 = 20%; Supplementary Table S1). No neurofibroma formation was observed upon gross dissection of these 7 mice.

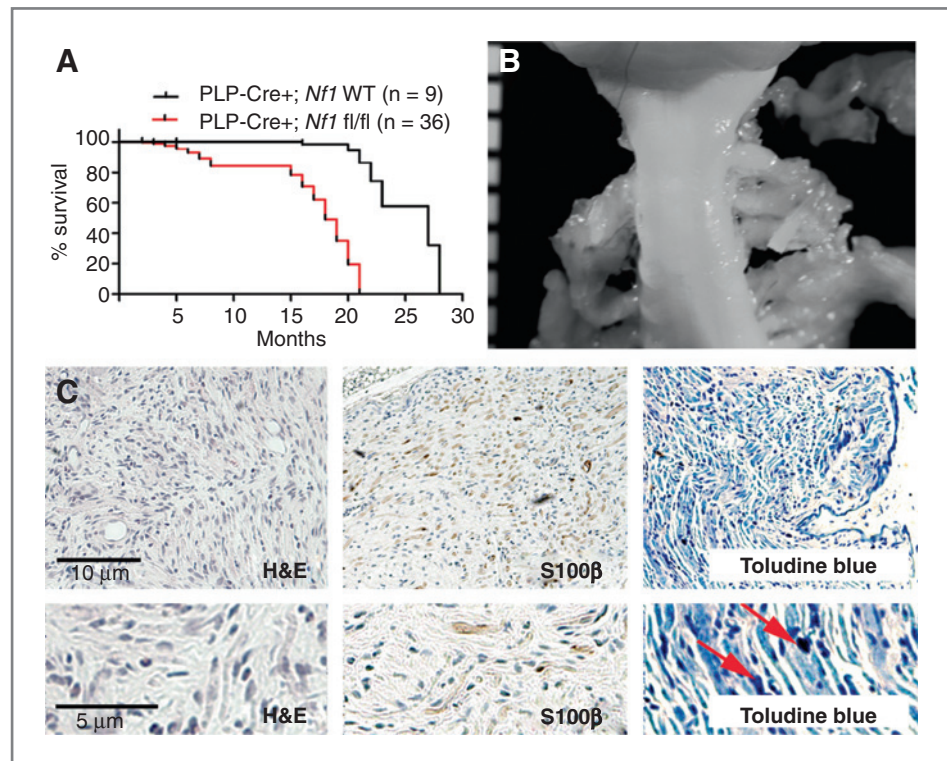
The remaining *PlpCre;Nf1fl/fl* animals (29/36; 80%) required sacrifice between 15 and 21 months of age. Littermate *PlpCre;Nf1wt* controls (designated "WT controls" or wild type throughout the manuscript) remained healthy. On gross dissection these *PlpCre;Nf1fl/fl* animals had enlarged peripheral nerves associated with paraspinal tumors at cervical (Fig. 1B) and thoracic spinal levels. Sixty-seven percent (4 of 6) of mice

in which full neuroaxis dissection was carried out also had paraspinal tumors within the lumbar/sacral regions (Supplementary Table S1). Grading and classification of tumors used GEM nerve sheath classification (28). GEM neurofibromas Grade I are defined as tumors with histological features similar to those of human neurofibromas; hypocellular with abundant matrix and collagen fibers, minimal cell atypia and rare mitosis. There are often intermixed nerve axons and mast cells present. All paraspinal tumors in the *PlpCre;Nf1fl/fl* model were GEM Grade I neurofibromas. On histological analysis, they showed low cellularity, stromal matrix between the cells, S100 β + myelinating Schwann cells, and mast cell infiltration (Fig. 1C).

Peripheral nerve sheath tumor formation after perinatal or adult tamoxifen exposure in *PLP-Cre;Nf1fl/fl* mice

One in 5 *PlpCre;Nf1fl/fl* mice developed GEM Grade III peripheral nerve sheath tumor (PNST; Supplementary Table S1 and Supplementary Fig. S1). Similar to human malignant peripheral nerve-sheath tumor (MPNST), GEM Grade III PNST are densely cellular tumors with marked anaplasia, high nuclear/cytoplasmic ratio, and frequent mitoses (Supplementary Fig. 1A–C, right). Tumors arose in the abdomen, at the base of the tail, or in hindlimbs after either perinatal or adult loss of *Nf1*. Clear relationships to lower grade neurofibroma and/or proximity to S100+ cells enabled classification as GEM PNST (Supplementary Fig. S1A, right insert).

Figure 1. Perinatal loss of *Nf1* mice causes two phases of mortality and late neurofibroma formation. A, Kaplan–Meier survival curve ($P < 0.0001$). B, gross dissection of cervical spinal cord with DRG-associated small GEM Grade I neurofibromas at each dorsal root in a *PlpCre+;Nf1fl/fl* animal at 18 months of age. Ruler shows 1 mm markings. C, tissue sections of GEM Grade I neurofibroma in *PlpCre+;Nf1fl/fl* animal after perinatal tamoxifen. Top panels are magnified 10 \times ; bottom panels are magnified 25 \times . Red arrows highlight mast cells.



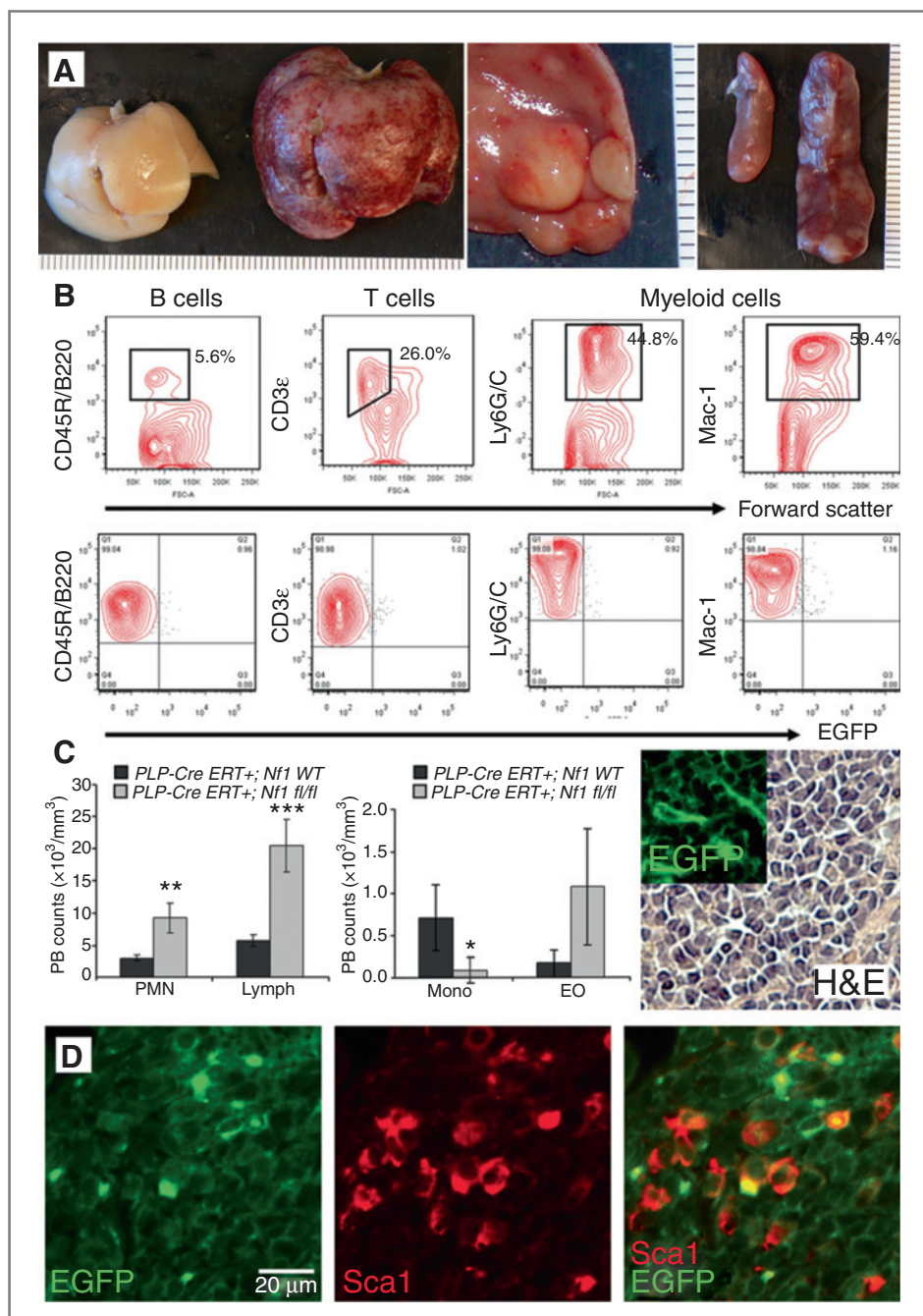


Figure 2. Perinatal *Nf1* loss causes reactive hyperplasia of hematopoietic cells. **A**, left, wild type liver; middle, *Nf1*^{fl/fl} enlarged liver with white masses; right, enlarged *Nf1*^{fl/fl} spleen with white masses (right) compared with a wildtype spleen (left). Rulers show 1 mm markings. **B**, flow cytometric analysis of splenocytes from *PLP-Cre ERT+;Nf1fl/fl;EGFP+* mice, analyzed for content of B (CD45R/B220), T (CD3ε), and myeloid cells (Ly6G/C and Mac-1). All were EGFP⁻. **C**, peripheral blood counts from total CBC and Blood Smear Counts show increased PMN (**, $P = 0.0026$) and lymphocytes (LY; ***, $P = 0.0006$), and decreased monocytes (MO; *, $P = 0.0347$) of *PLP-CreERT+;Nf1fl/fl* animals compared with age-matched littermate controls but not eosinophils (EO). **Right**, H&E stain and EGFP⁺ (insert) cells within a liver mass. Insert and H&E are at the same magnification (40 \times). **D**, double labeled Sca1⁺ (red) and EGFP⁺ (green) cells (40 \times). Round cells of possible lymphohematopoietic lineage are EGFP negative.

Perinatal tamoxifen exposure in *PlpCre;Nf1fl/fl* mice causes reactive hyperplasia of hematopoietic cells

Endogenous Plp is expressed in spleen and thymus as well as glial cells (29). Therefore, this *PlpCre* driver could be expressed within hematopoietic cell populations. Postnatal (P1–3) tamoxifen injections within *PlpCre;Nf1fl/fl* animals caused development of tumors resulting from extramedullary expansion of lymphoid and myeloid cell populations in 36% of the animals examined. Seven developed early (by 5 to 7 months of age) and 7 animals contained hematopoietic-containing tumors at necropsy in the context of complica-

tions arisen from neurofibroma formation (15 to 22 months of age). Enlarged organs with solid white lesions were noted within the liver, spleen, lung, kidney, lacrimal gland, and lymph nodes within the abdominal cavity, neck, inguinal, and axillary regions (Fig. 2A). Within the subset of animals that developed these tumors, splenomegaly, a prominent finding in a number of hematopoietic abnormalities including JMML, was common (Fig. 2A, right). These animals often suffered dermatitis of the face and neck. While eczema is common in JMML, these dermal lesions overlaid neurofibromas deep within the tissue.

To characterize the hematopoietic lineage within these tumors, flow cytometry analysis of splenocytes or abdominal masses from *PlpCre;Nf1^{fl/fl};EGFP⁺* mice was carried out. Tumors were composed of a heterogeneous hematopoietic cell population (B cells, T cells, and myeloid cells), which were EGFP negative (Fig. 2B). We examined the peripheral blood of wild type and *PlpCre;Nf1^{fl/fl}* animals at 7 months of age. Total CBC and Blood Smear Counts showed an increase in polymorphic mononuclear cells (PMN; $P = 0.0026$) and lymphocytes (LY; $P = 0.0006$), with a decrease in monocytes (MO; $P = 0.0347$) in *PLPCre;Nf1^{fl/fl}* animals compared with age-matched littermate controls (Fig. 2C).

Histological analysis of tumor sections revealed the presence of EGFP⁺ cells morphologically distinct from the lympho-myeloid infiltrate (Fig. 2D). EGFP⁺ cells were spindle shaped, infiltrated the lymphohematopoietic tissue and some EGFP⁺ cells expressed Sca-1, a recognized marker of mesenchymal cells and progenitors with hematopoietic supportive ability in C57Bl/6 and FVB/N background mice (30–32) (Fig. 2D). Flow cytometry studies of adult *PlpCre* blood and bone marrow confirmed the absence of EGFP⁺ within progenitor and mature hematopoietic cells (data not shown). These data indicate that loss of *Nf1* within this model causes

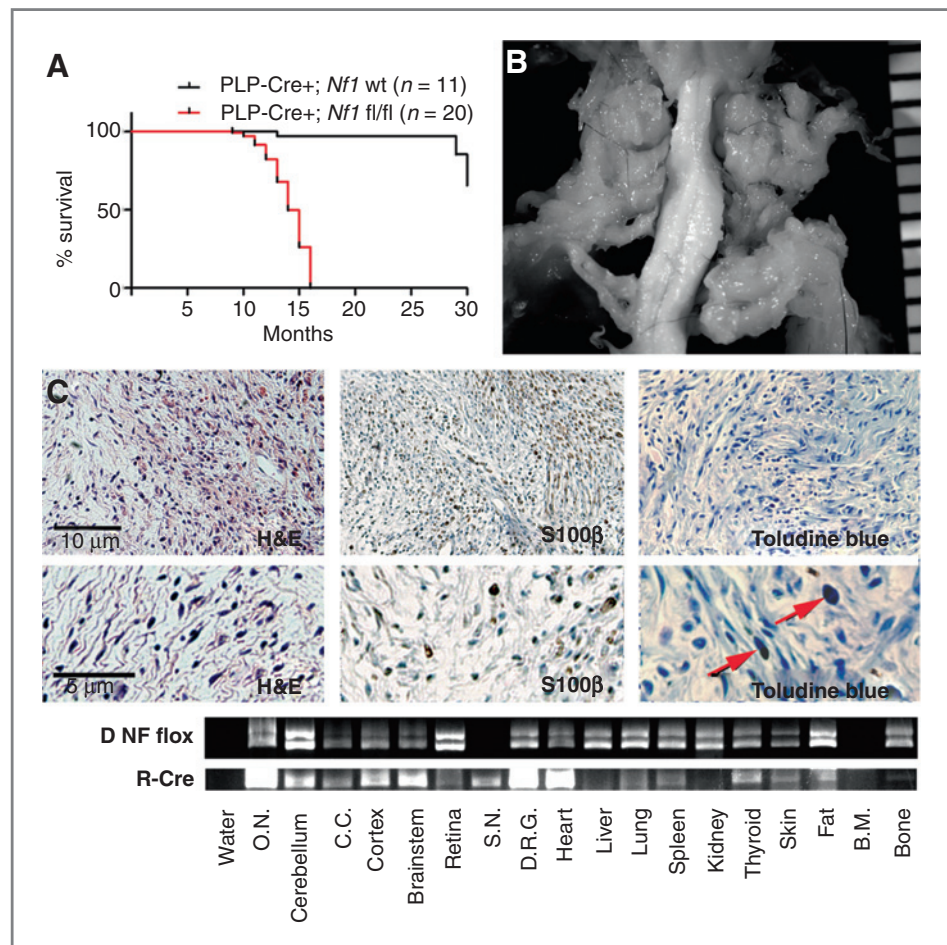
an unidentified hematopoietic proliferative disorder distinctive from JMML. Furthermore, because EGFP⁺ recombination did not occur within hematopoietic-lineage cells, cell hyperproliferation occurs in a noncell autonomous fashion after perinatal (P1–3) loss of *Nf1* within *PlpCre⁺* nonhematopoietic, stromal cells.

Adult loss of *Nf1* can cause neurofibroma formation

To test whether loss of *Nf1* within adult animals can elicit tumor phenotype(s) *in vivo*, we injected adult (8 to 10 weeks) *PlpCre;Nf1^{fl/fl}* mice with tamoxifen. All mutant mice required sacrifice between 7 and 15 months of age (5 to 13 months post-tamoxifen exposure) due to paralysis, whereas littermate *WT* controls remained healthy (Fig. 3A; $P < 0.0001$). Hematopoietic tumors were evident in 3 of 20 (15%) of adult tamoxifen-injected *PlpCre;Nf1^{fl/fl}* animals on gross dissection.

Gross dissections were carried out on the neuroaxis of 20 *PlpCre;Nf1^{fl/fl}* animals. All had tumors associated with peripheral nerves and DRGs (Supplementary Table S1), and cranio-facial nerves. Figure 3B displays representative tumors associated with spinal and peripheral nerves of a *PlpCre;Nf1^{fl/fl}* animal, diagnosed as GEM Grade I neurofibromas after paraffin embedding and staining with H&E (Fig. 3C). Similar to

Figure 3. Adult Tamoxifen exposure in *PlpCre;Nf1^{fl/fl}* mice causes neurofibroma formation. A, Kaplan–Meyer survival curve ($P < 0.0001$). B, gross dissection of cervical spinal cord with GEM Grade I neurofibromas in a *PlpCre⁺;Nf1^{fl/fl}* animal. Ruler shows 1 mm markings. C, tissue sections of a GEM Grade I neurofibroma in a *PlpCre⁺;Nf1^{fl/fl}* animal after adult tamoxifen. Top panels are magnified 10 \times ; bottom panels are magnified 25 \times . Red arrows highlight mast cells. D, PCR analysis shows the *Nf1* floxed allele (NF flox) and the recombined Cre allele (R-Cre). Each lane contains 1 μ g of DNA. O.N., optic nerve; C.C., corpus callosum; S.N., sciatic nerve; DRG, dorsal root ganglia; B.M., bone marrow.



perinatal *PlpCre;Nf1fl/fl* neurofibromas, these displayed low cellularity with increased stroma between the cells. The neurofibromas contained characteristic S100 β + cells and mast cell infiltration (Fig. 3C).

Recombination was examined by PCR analysis (Fig. 3D). As expected, recombination was noted within the brain and peripheral nervous system (sciatic nerve and dorsal root ganglia). Recombination was also detected in the heart, lung, spleen, thyroid, skin, fat, and bone. Recombination was absent within the liver, kidney, and bone marrow. EGFP+ cells were present within peripheral nerves throughout the body (data not shown). Organ-specific EGFP+ cells were also noted within the heart, lung, thyroid, and spleen (Supplementary Fig. 2), likely accounting for some of the recombination observed.

Comparison of neurofibroma formation after perinatal or adult tamoxifen exposure in *PlpCre;Nf1fl/fl* mice

When compared with 15-month-old wild type controls (Fig. 4A), *PlpCre* animals after either perinatal (Fig. 4B) or adult (Fig. 4C) loss of *Nf1* show neurofibroma formation in cranial nerves (Fig. 4, top panel), DRGs, and peripheral nerves (Fig. 4B & C). Cranial nerves commonly developed neurofibromas extending into the face, neck, and tongue. These tumors sometimes compressed the brainstem, which resulted in head tilt and circling behavior (Fig. 4B asterisks). Neurofibromas were larger in mice injected with tamoxifen as adults, likely accounting for earlier animal lethality. Some tumors compressed the spinal cord; however, commonly tumors surrounded the DRG and extended laterally along peripheral

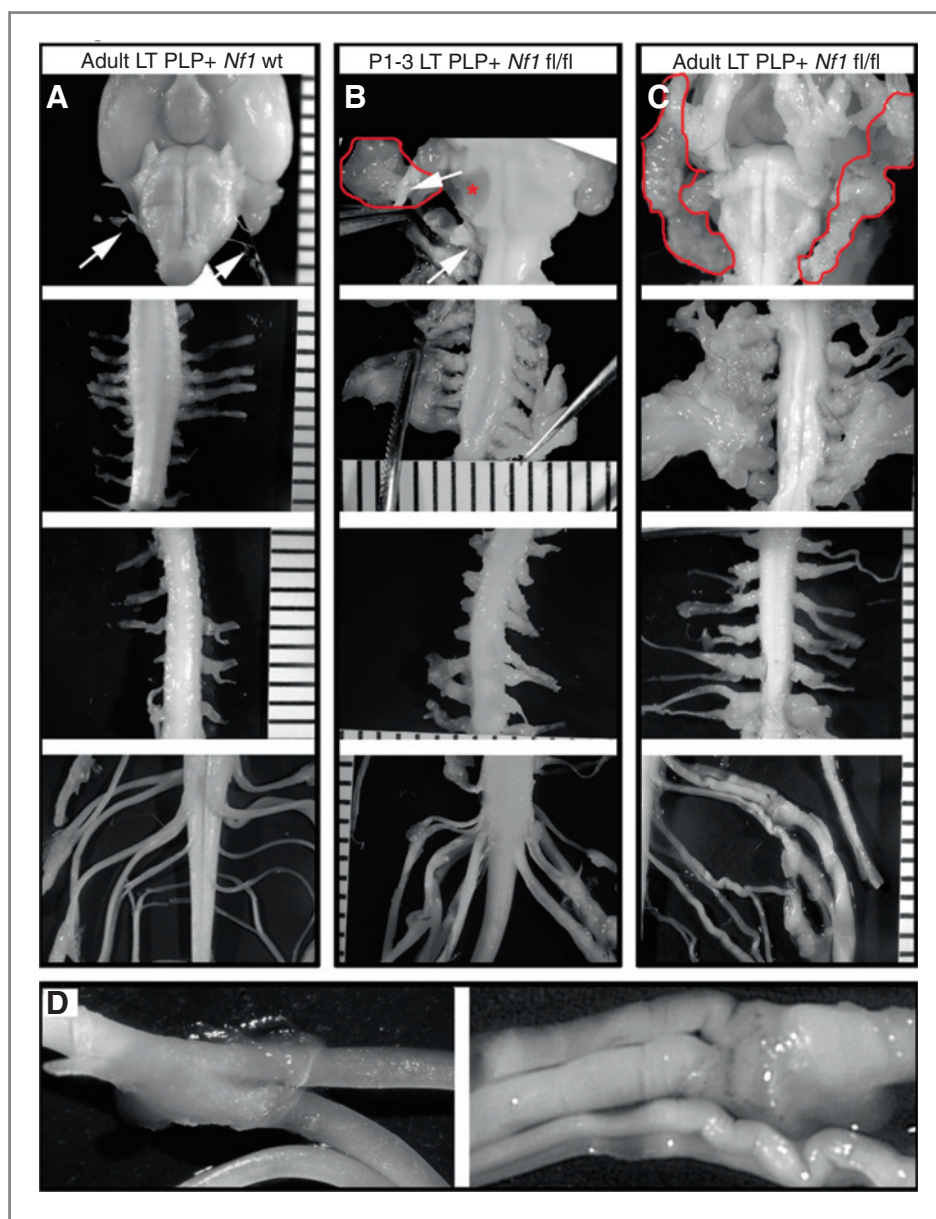
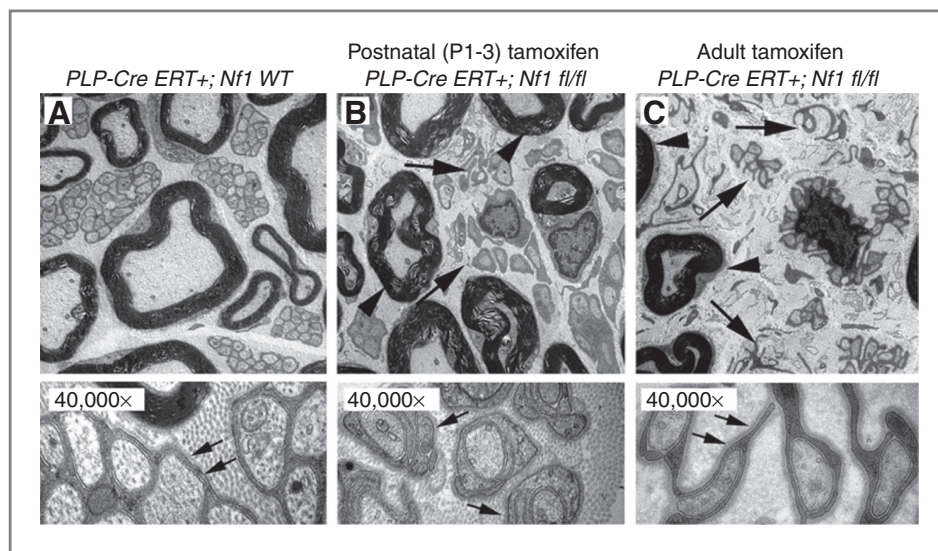


Figure 4. Neurofibroma formation is predominant within the peripheral nerves and DRGs at cervical spinal levels. Gross micrographs show age-matched 12-month-old (A) *PlpCre;WT*, (B) P1–3 tamoxifen-injected *PlpCre;Nf1fl/fl*, and (C) adult tamoxifen-injected *PlpCre;Nf1fl/fl* animals. Brainstem (top row), cervical (second row), thoracic (third row), and lumbar/sacral (fourth row) spinal cord. Ruler shows 1 mm markings. Arrows (A & B), cranial nerves emerging from the brainstem. Red lines (B & C), facial neurofibromas developed from cranial nerves. Red asterisk (* in B), compression of the brainstem resulting from cranial nerve neurofibroma (pulled away with forceps to show compression). In cervical neurofibroma images (B & C; second row) forceps slightly pulled the nerves from the spinal cord to visualize tumors. Adult tamoxifen-injected *PlpCre;WT* and *PlpCre;Nf1fl/fl* peripheral nerves of the cauda equine are shown enlarged in D.

Figure 5. Disrupted Remak bundles in *PlpCre;Nf1fl/fl* nerves. Electron micrographs of the saphenous nerves of 12-month-old (A) *PlpCre+;WT* control, (B) P1–3 tamoxifen-injected *PlpCre+;Nf1fl/fl*, and (C) adult tamoxifen-injected *PlpCre+;Nf1fl/fl* animals. Large arrows in B & C highlight Remak bundle disruption; arrowheads highlight myelin sheaths in B & C. 4,000 \times , top panels. 40,000 \times , bottom panels. Schwann cell cytoplasmic processes are identified by their continuous basal lamina (small arrows, lower panels).



nerves. *PlpCre;Nf1fl/fl* cauda equina nerves also showed enlargement and nerves often showed kinks (Fig. 4D).

Remak bundle disruption within *PlpCre;Nf1fl/fl* saphenous nerves

Electron microscopy compared saphenous nerves of 12-month-old *PlpCre+;Nf1wt* control (Fig. 5A), postnatal (P1–3) tamoxifen-injected *PlpCre+;Nf1fl/fl* (Fig. 5B), and adult tamoxifen-injected *PlpCre+;Nf1fl/fl* animals (Fig. 5C) to determine whether loss of *Nf1* within *PlpCre+* cells affects Remak bundles. Similar to other mouse neurofibroma models, myelination of large diameter axons appeared normal after either perinatal or adult loss of *Nf1* whereas perinatal or adult tamoxifen exposure caused Remak bundle disruption (Fig. 5B & C). Thus many small caliber axons were found in a one to one relationship with an attendant axon while other Schwann cells were dissociated from axons completely, and pathologically wrapped collagen.

PlpCre targets multiple glial cell types in the peripheral nervous system: identification using EGFP

To define cells targeted by the *PlpCre* driver, we analyzed *PlpCre; CMB- β actin loxP EGFP* flanked chloramphenicol acetyltransferase (CAT) mice one-day-post last tamoxifen injection (i.e., 4-days-post tamoxifen introduction). The percent of EGFP+; DAPI+ nonneuronal cells was higher in DRG and sciatic nerve after perinatal injection compared with adult tamoxifen injection (Fig. 6A left). The development of immature Schwann cells into myelinating and nonmyelinating nerve Schwann cells is incomplete in perinatal life (12). Therefore we focused on defining cell types expressing *PlpCre* (EGFP+ staining) in adult mice. EGFP was detected in 7% of the nonneuronal cells within cervical DRG and 18% of cells within the adult sciatic nerve. The percentage of EGFP+; S100 β + satellite cells in the DRG was 11%; and myelinating Schwann cells in sciatic nerve = 25% (Fig. 6A right, & 6B). S100 β + cells in the sciatic nerve were myelinating Schwann cells as confirmed by double labeling with antiperiaxin (data

not shown). In neurofibromas, months after tamoxifen exposure *PlpCre;Nf1fl/fl* cells continue to show EGFP double labeling with S100 β + (Fig. 6B).

In wild type mice, the percentage of double-labeled EGFP+; GFAP+ cells 4 days after tamoxifen within the DRG was 34%; and sciatic nerve = 0% (Fig. 6A right, & Fig. 6C). Thus, the *PlpCre* construct is not active within the GFAP+ nonmyelinating cells in the peripheral nerve. In neurofibromas, months after tamoxifen exposure *PlpCre;Nf1fl/fl* cells did not express GFAP (Fig. 6C).

There were no EGFP+;p75+ wild type satellite cells within the DRG 4 days after tamoxifen (Fig. 6D). EGFP+;p75+ cells were present in the sciatic nerve (Fig. 6D). EGFP+ cells (59% in DRG, & 41% in sciatic nerve) double-labeled with the Schwann cell and satellite cell marker glutathione synthase (GS) (Fig. 6A right). Thus the *PlpCre* driver targets myelinating S100 β + Schwann cells within the sciatic nerve, and unidentified p75+ cells. Within the DRG, all EGFP+ cells had the morphology of satellite cells, with distinctive cell processes wrapping around DRG neurons.

Rapid onset of proliferation in *Nf1* mutant cells

We noted that the numbers of EGFP+ cells in *PlpCre;Nf1fl/fl* dorsal root ganglia seemed to increase over time (Fig. 7A). Quantification of EGFP+ cells at 1, 7, and 28 days following tamoxifen injection in the sciatic nerve showed that beginning 1 day after the final tamoxifen injection the numbers of EGFP+ cells were significantly increased in *PlpCre;Nf1fl/fl* as compared with wild type (Fig. 7B). We monitored cells in the S-phase of the cell cycle with BrdU immunostaining. Many nerve and neurofibroma EGFP+ cells were BrdU+, likely accounting at least in part for the observed increase in cell number (Fig. 7C).

Discussion

In this study we found that both postnatal (P1–3) and adult loss of *Nf1* using the *PlpCre* driver cause GEM-grade I

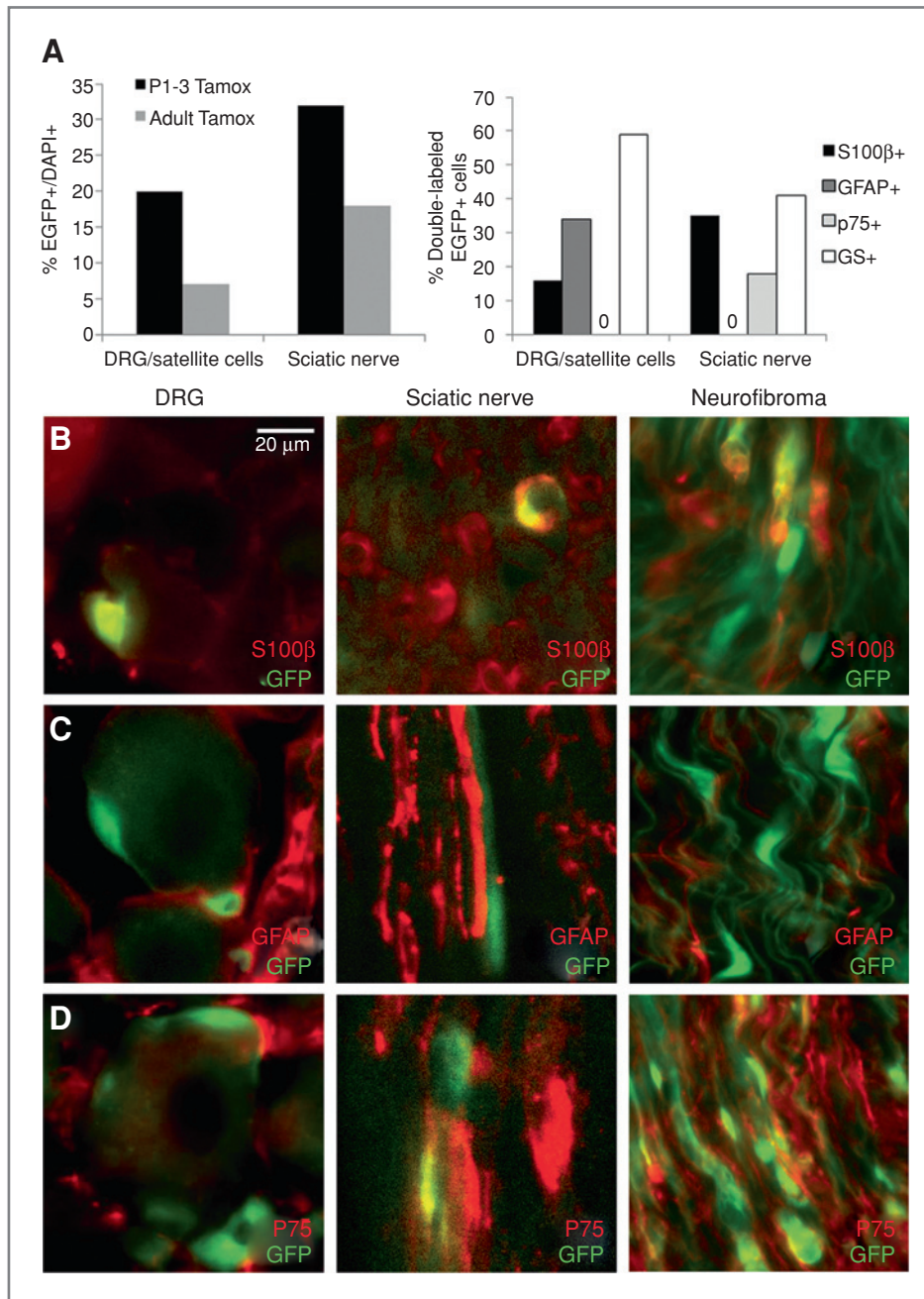


Figure 6. EGFP+ cells after tamoxifen injection in *PlpCre*+ animals. **A**, graph (left) indicates percentages of EGFP+/DAPI+ cells in sciatic nerve and DRG/satellite cells and (right) the percent of EGFP+ recombined cells that double labeled with S100β, GFAP, p75, or GS. **B**, double immunolabeling (40×) shows EGFP+/S100β+ cells within the DRG or sciatic nerve one-day-post Tamoxifen. **C**, EGFP+/GFAP+ cells are present in the DRG but not sciatic nerve. **D**, EGFP+/p75+ cells are absent in the DRG and present in sciatic nerve. Immunohistochemistry in neurofibromas after adult tamoxifen exposure within the *PlpCre;Nf1fl/fl* model shows EGFP double labeling with S100β+ (**B**) and p75 (**D**) but not GFAP+ (**C**).

neurofibroma tumor formation. The models differ in the timing of neurofibroma formation, in the size of the neurofibromas generated, and in prevalence of hematopoietic manifestations. We found that myelinating Schwann cells, p75+ cells, and satellite cells are targeted by the inducible *PlpCre* driver. Our results support previous studies indicating that loss of *Nf1* in subpopulations of nerve Schwann cell lineage cells cause neurofibroma formation, and extend these studies by showing that acute *Nf1* loss, after organogenesis and cell differentiation, can be tumorigenic.

We identified EGFP+ cells to identify possible tumor cells of origin in the *PlpCre* model. Tamoxifen exposure induced

peripheral nervous system recombination, as judged by EGFP+ cells, in satellite cells in the DRG (S100β+ or GFAP+) with the characteristic morphology of satellite cells, closely wrapping DRG cell bodies. In *DhhCre;Nf1fl/fl* mice, satellite cells do not show recombination, yet neurofibromas form (24). While not definitive, the combination of the two models does not support a role for satellite cells in mouse neurofibroma formation; however, the possibility that satellite cells are important for neurofibroma formation in some settings whereas not in others cannot be excluded.

Most EGFP+ cells in adult peripheral nerves were S100β+ (myelinating) Schwann cells. This result is expected, as

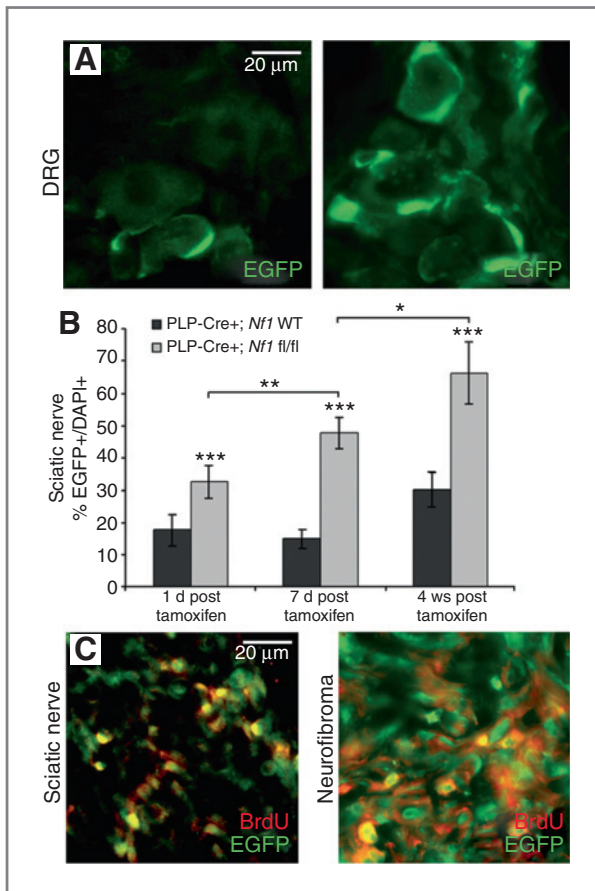


Figure 7. EGFP⁺ cells proliferate in *PlpCre*⁺ animals. EGFP⁺ cells (green; 40 \times) within the DRG one-day-post last Tamoxifen injection (A, left) and 15-months-post Tamoxifen (A, right) in *PlpCre*;*Nf1*^{fl/fl} animals. B, quantification of the EGFP⁺ population in sciatic nerves of *PlpCre*;*Nf1*^{fl/fl} and littermate wild type animals ($n = 3-5$ per time point per genotype). The total% EGFP⁺/DAPI⁺ cells were calculated after times after tamoxifen injection. BrdU immunostaining (40 \times) colocalizes in EGFP⁺ cells at 4-weeks-post Tamoxifen injection (C, left) and within a neurofibroma (C, right). * $P < 0.01$; ** $P < 0.001$; *** $P < 0.00001$.

endogenous Plp is a characteristic of myelinating Schwann cells in adult peripheral nerve (33). At the EM level, *Nf1* loss did not dramatically alter myelination.

Remak bundle disruption is a characteristic feature of all neurofibroma models (22–24, 34). When the nonmyelinated Schwann cell population was examined, no EGFP⁺/GFAP⁺ nonmyelinating Schwann cells were identified. These data are surprising as electron microscopy shows disruption of the association between axons and nonmyelinating Schwann cells in the *PlpCre*;*Nf1*^{fl/fl} model. We conclude that *Nf1* loss within GFAP⁺ cells is not necessary for Remak bundle disruption in the *PlpCre*;*Nf1*^{fl/fl} model.

We identified EGFP⁺;p75⁺ cells in peripheral nerve. These may be a subpopulation of GFAP-negative nonmyelinating cells, and/or an as-yet unidentified population(s) in adult peripheral nerve. Zheng and colleagues (2008) proposed that the p75⁺ nonmyelinating cell population was the cell of origin for neurofibroma formation (23). The present study eliminates

the GFAP⁺ nonmyelinating Schwann cell as the tumor-initiating cell. It is possible that neurofibroma formation results from the p75⁺/GFAP-negative cells in peripheral nerve, and/or that loss of *Nf1* within mature myelinating Schwann cells have noncell autonomous effect(s) that promote tumor formation—similar to the noncell autonomous effect on hematopoietic cells when *Nf1* is lost within stromal cells.

Perinatal tamoxifen injection into *PlpCre*;*Nf1*^{fl/fl} mice resulted in GEM grade I neurofibroma formation that resulted in morbidity at 15 to 23 months old. In contrast, adult loss of *Nf1* resulted in large neurofibromas, which caused morbidity beginning 5 months post-tamoxifen introduction. We considered the possibility that recombination occurs in more cells when tamoxifen-induced recombination occurs in adults. However, twice as many cells in sciatic nerve and three times as many in the DRG were EGFP⁺ in pups as compared with adult mice. Therefore together with previous studies showing that loss of *Nf1* in most developing Schwann cells leads to robust neurofibroma formation (22–24) we conclude that cells exist in the adult peripheral nervous system that remain susceptible to neurofibroma formation, and that the susceptible population(s) may be enriched in adult and embryonic nervous systems.

A study submitted by Le and colleagues confirms our observation that neurofibromas can form after perinatal or adult loss of *Nf1*. However, while they identified small neurofibromas at the thoracic and lumbo-sacral levels after adult loss of *Nf1*, we generated large neurofibromas throughout the neuroaxis. Some differences between the two studies may account for the slightly different findings. Le and colleagues provided 4 mg tamoxifen (2 mg twice daily) by oral gavage to adult mice for 5 days, whereas we dosed 1 mg twice daily by i.p. injection for 3 days. It is also possible that the different phenotypes result from the different tamoxifen-inducible *PlpCre* driver lines used in the two studies. This difference may well account for the absence of hematopoietic lesions in their system. Most importantly, our data do not support the idea that there is a critical window for neurofibroma formation.

Mast cells, and other hematopoietic cells, showed <1% recombination in *PlpCre*;*Nf1*^{fl/fl} mice, yet neurofibroma formation was robust. While *Krox20Cre*;*Nf1*^{fl/fl} mice show hyperplasia within the DRG, neurofibroma development required an *Nf1*^{+/-} background attributed to *Nf1*^{+/-} mast cells (22, 35). *DhhCre*;*Nf1*^{fl/fl} animals develop neurofibromas when only Schwann cell lineage cells are *Nf1* mutant (24), and the *PlpCre*;*Nf1*^{fl/fl} model is similar in that a heterozygous background is not necessary for neurofibroma formation.

The peripheral blood of *PlpCre*;*Nf1*^{fl/fl} mice showed a decrease in monocytes with a relative increase in lymphocytes and polymorphonuclear (PMN). In contrast, *Nf1* loss driven by Mx1-Cre causes a mouse disorder similar to human juvenile myelomonocytic leukemia (JMML), with hyperproliferation of all hematopoietic cell types and progressive myeloproliferative disorder (36, 37, 38). Flow cytometry and immunohistochemistry showed that the *PlpCre* transgene did not cause *Nf1* loss in cells of hematopoietic origin. Rather, EGFP⁺ cells within these tumors had a stromal/mesenchymal appearance, and some double-labeled with Sca-1. EGFP expression did not

colocalize with the expression of hematopoietic lineage markers or c-kit (data not shown), indicating that recombined EGFP+ cells had a nonhematopoietic and mesenchymal origin (30, 39).

The idea that *Nf1* loss can affect tumorigenesis in a noncell autonomous fashion (e.g., myelinating cells acting upon other cells in the nerve) is thus supported by analogy to the formation of hematopoietic lesions within the *PlpCre;Nf1^{fl/fl}* animals, in which mutant stromal cells after either perinatal or adult tamoxifen-induced *Nf1* loss, cause lymphoid and myeloid proliferation. However we cannot exclude the possibility that neurofibroma formation requires *Nf1* loss of function in a small population of stem/progenitor-like cells that remain unidentified by our analysis, or induces expression of chemoattractants that result in massive tissue infiltration by hematopoietic cells. In either event, neurofibroma formation is not restricted to loss of *Nf1* in embryonic life, but can be triggered by *Nf1* loss throughout life.

References

- Friedman JM. Epidemiology of neurofibromatosis type 1. *Am J Med Genet* 1999;891:1-6.
- Boyd KP, Korf BR, Theos A. Neurofibromatosis type 1. *J Am Acad Dermatol* 2009;611:1-14.
- Rosenfeld A, Listerick R, Charrow J, Goldman S. Neurofibromatosis type 1 and high-grade tumors of the central nervous system. *Childs Nerv Syst* 2010;265:663-7.
- Emanuel PD, Bates LJ, Castleberry RP, Gualtieri RJ, Zuckerman KS, et al. Selective hypersensitivity to granulocyte-macrophage colony-stimulating factor by juvenile chronic myeloid leukemia hematopoietic progenitors. *Blood* 1991;77:925-9.
- Niemeyer CM, Arico M, Basso G, Biondi A, Cantu Rajnoldi A, Creutzig U, et al. Quantitative effects of Nf1 inactivation on in vivo hematopoiesis. *Blood* 1997;89:3534.
- Side LE, Emanuel PD, Taylor B, Franklin J, Thompson P, Castleberry RP, et al. Mutations of the NF1 gene in children with juvenile myelomonocytic leukemia without clinical evidence of neurofibromatosis, type 1. *Blood* 1998;92:267-72.
- Woodruff JM. Pathology of tumors of the peripheral nerve sheath in type 1 neurofibromatosis. *Am J Med Genet* 1999;891:23-30.
- Serra E, Puig S, Otero D, Gaona A, Kruyer H, Ars E, et al. Confirmation of a double-hit model for the NF1 gene in benign neurofibromas. *Am J Hum Genet* 1997;61:512-9.
- Serra E, Ars E, Ravella A, Sánchez A, Puig S, Rosenbaum T, et al. Somatic NF1 mutational spectrum in benign neurofibromas; mRNA splice defects are common among point mutations. *Hum Genet* 2001;108:416-29.
- Maertens O, Brems H, Vandesompele J, De Raedt T, Heyns I, Rosenbaum T, et al. Comprehensive NF1 screening on cultured Schwann cells from neurofibromas. *Hum Mutat* 2006;27:1030-40.
- Dong Z, Sinanan A, Parkinson D, Parmantier E, Mirsky R, Jessen KR, et al. Schwann cell development in embryonic mouse nerves. *J Neurosci Res* 1999;56:334-48.
- Jessen KR, Mirsky R. The origin and development of glial cells in peripheral nerves. *Nat Rev* 2005;6:671-82.
- Bixby S, Kruger GM, Mosher JT, Joseph NM, Morrison SJ, et al. Cell-intrinsic differences between stem cells from different regions of the peripheral nervous system regulate the generation of neural diversity. *Neuron* 2002;35:643-56.
- Joseph NM, Mosher JT, Buchstaller J, Snider P, McKeever PE, Lim M, et al. The loss of Nf1 transiently promotes self-renewal but not tumorigenesis by neural crest stem cells. *Cancer Cell* 2008;132:129-40.
- Kléber M, Lee HY, Wurdak H, Buchstaller J, Riccomagno MM, Ittner LM, et al. Neural crest stem cell maintenance by combinatorial Wnt and BMP signaling. *J Cell Biol* 2005;169:309-20.
- Morrison SJ, White PM, Zock C, Anderson DJ. Prospective identification, isolation by flow cytometry, and in vivo self-renewal of multipotent mammalian neural crest stem cells. *Cell* 1999;965:737-49.
- Nagoshi N, Nagoshi N, Shibata S, Kubota Y, Nakamura M, Nagai Y, et al. Ontogeny and multipotency of neural crest-derived stem cells in mouse bone marrow, dorsal root ganglia, and whisker pad *Cell Stem Cell* 2008;2:392-403.
- Mirsky R, Woodhoo A, Parkinson DB, Arthur-Farraj P, Bhaskaran A, Jessen KR, et al. Novel signals controlling embryonic Schwann cell development, myelination and dedifferentiation. *J Peripheral Nerv Syst* 2008;13:122-35.
- Brannan CI, Perkins AS, Vogel KS, Ratner N, Nordlund ML, Reid SW, et al. Targeted disruption of the neurofibromatosis type-1 gene leads to developmental abnormalities in heart and various neural crest-derived tissues. *Genes Dev* 1994;8:1019-29.
- Jacks T, Shih TS, Schmitt EM, Bronson RT, Bernards A, Weinberg RA. Tumour predisposition in mice heterozygous for a targeted mutation in Nf1. *Nat Genet* 1994;7:353-61.
- Gitler AD, Zhu Y, Ismat FA, Lu MM, Yamauchi Y, Parada LF, et al. Nf1 has an essential role in endothelial cells. *Nat Genet* 2003;331:75-9.
- Zhu Y, Ghosh P, Charnay P, Burns DK, Parada LF, et al. Neurofibromas in NF1; Schwann cell origin and role of tumor environment. *Science* 2002;296:920-2.
- Zheng H, Chang L, Patel N, Yang J, Lowe L, Burns DK, et al. Induction of abnormal proliferation by nonmyelinating Schwann cells triggers neurofibroma formation. *Cancer Cell* 2008;13:117-28.
- Wu J, Williams JP, Rizvi TA, Kordich JJ, Witte D, Meijer D, et al. Plexiform and dermal neurofibromas and pigmentation are caused by Nf1 loss in desert hedgehog-expressing cells. *Cancer Cell* 2008;13:105-16.
- Mallon BS, Shick HE, Kidd GJ, Macklin WB. Proteolipid Promoter Activity Distinguishes Two Populations of NG2-Positive Cells throughout Neonatal Cortical Development. *J Neurosci* 2002;22:876-85.
- Doerflinger NH, Macklin WB, Popko B. Inducible site-specific recombination in myelinating cells. *Genesis* 2003;35:63-72.
- Nakamura T, Colbert MC, Robbins J. Neural crest cells retain multipotential characteristics in the developing valves and label the cardiac conduction system. *Circ Res* 2006;9812:1547-54.
- Stemmer-Rachamimov AO, Louis DN, Nielsen GP, Antonescu CR, Borowsky AD, Bronson RT, et al. Comparative pathology of nerve

Disclosure of Potential Conflicts of Interest

No potential conflicts of interest were disclosed.

Acknowledgments

We thank Brian Popko (University of Chicago) for providing the inducible *Plp-Cre-ERT* mice.

Grant Support

The DAMD Program on Neurofibromatosis (W81XWH-06-1-0114 to T.A. Rizvi and N. Ratner) and NIH R01-NS28840 (N. Ratner) supported this work. NIH NRSA (T32CA117846) and National Multiple Sclerosis Society (FG1762A1/1) supported D.A. Mayes.

The costs of publication of this article were defrayed in part by the payment of page charges. This article must therefore be hereby marked *advertisement* in accordance with 18 U.S.C. Section 1734 solely to indicate this fact.

Received December 21, 2010; revised March 2, 2011; accepted March 17, 2011; published OnlineFirst May 6, 2011.

- sheath tumors in mouse models and humans. *Cancer Res* 2004;64:3718–24.
29. Feng JM, Fernandes AO, Bongarzone ER, Campagnoni CW, Kampf K, Campagnoni AT, et al. Expression of soma-restricted proteolipid/DM20 proteins in lymphoid cells. *J Neuroimmunol* 2003;144:9–15.
30. Morikawa S, Mabuchi Y, Kubota Y, Nagai Y, Niibe K, Hiratsu E, et al. Prospective identification, isolation, and systemic transplantation of multipotent mesenchymal stem cells in murine bone marrow. *J Exp Med* 2009;206:11:2483–96.
31. Gao J, Yan XL, Li R, Liu Y, He W, Sun S, et al. Characterization of OP9 as authentic mesenchymal stem cell line. *J Genet Genomics* 2010;377:475–82.
32. Peister A, Mellad JA, Larson BL, Hall BM, Gibson LF, Prockop DJ, et al. Adult stem cells from bone marrow MSCs isolated from different strains of inbred mice vary in surface epitopes, rates of proliferation, and differentiation potential. *Blood* 2004;103:1662–8.
33. Gupta SK, Pringle J, Poduslo JF, Mezei C. Levels of proteolipid protein mRNAs in peripheral nerve are not under stringent axonal control. *J Neurochem* 1991;56:1754–62.
34. Ling BC, Wu J, Miller SJ, Monk KR, Shamekh R, Rizvi TA, et al. Role for the epidermal growth factor receptor in neurofibromatosis-related peripheral nerve tumorigenesis. *Cancer Cell* 2005;71:65–75.
35. Yang FC, Ingram DA, Chen S, Zhu Y, Yuan J, Li X, et al. Nf1-deficient tumors require a microenvironment containing Nf1^{+/-} and c-kit-dependent bone marrow. *Cell* 2008;135:3:437–48.
36. Le DT, Kong N, Zhu Y, Lauchle JO, Aiyigari A, Braun BS, et al. Somatic inactivation of Nf1 in hematopoietic cells results in a progressive myeloproliferative disorder. *Blood* 2004;103:4243–50.
37. Zhang Y, Taylor BR, Shannon K, Clapp DW. Defective proliferative responses in B lymphocytes and thymocytes that lack neurofibromin. *J Clin Invest* 2001;108:5:709–15.
38. Kim TJ, Cariappa A, Iacomini J, Tang M, Shih S, Bernards A, et al. Defective proliferative responses in B lymphocytes and thymocytes that lack neurofibromin. *Mol Immunol* 2002;38:9:701–8.
39. Chan CK, Chen CC, Luppen CA, Kim JB, DeBoer AT, Wei K, et al. Endochondral ossification is required for haematopoietic stem-cell niche formation. *Nature* 2009;457:490–4.

Cancer Research

The Journal of Cancer Research (1916–1930) | The American Journal of Cancer (1931–1940)

Perinatal or Adult *Nf1* Inactivation Using Tamoxifen-Inducible *PlpCre* Each Cause Neurofibroma Formation

Debra A. Mayes, Tilat A. Rizvi, Jose A. Cancelas, et al.

Cancer Res 2011;71:4675-4685. Published OnlineFirst May 6, 2011.

Updated version	Access the most recent version of this article at: doi: 10.1158/0008-5472.CAN-10-4558
Supplementary Material	Access the most recent supplemental material at: http://cancerres.aacrjournals.org/content/suppl/2011/06/17/0008-5472.CAN-10-4558.DC1

Cited articles	This article cites 39 articles, 10 of which you can access for free at: http://cancerres.aacrjournals.org/content/71/13/4675.full.html#ref-list-1
Citing articles	This article has been cited by 3 HighWire-hosted articles. Access the articles at: /content/71/13/4675.full.html#related-urls

E-mail alerts	Sign up to receive free email-alerts related to this article or journal.
Reprints and Subscriptions	To order reprints of this article or to subscribe to the journal, contact the AACR Publications Department at pubs@aacr.org .
Permissions	To request permission to re-use all or part of this article, contact the AACR Publications Department at permissions@aacr.org .